COMPUTER METHODS IN APPLIED MECHANICS AND ENGINEERING 38 (1983) 185–202
NORTH-HOLLAND PUBLISHING COMPANY

A LUMPED CIRCUIT MODEL FOR A NONLINEAR INDUCTOR EXHIBITING DYNAMIC HYSTERESIS LOOPS AND ITS APPLICATION TO THE ELECTRIC CIRCUITS

Y. SAITO, H. SAOTOME and T. YAMAMURA
Department of Electrical Engineering, College of Engineering, Hosei University, Tokyo 184, Japan

Received 15 June 1982
Revised manuscript received 12 November 1982

Previously, modeling magnetodynamic fields, taking into account dynamic hysteresis loops, was proposed for predicting three-dimensional magnetodynamic fields in electromagnetic devices. This method is now applied to work out the lumped circuit model for a nonlinear inductor exhibiting dynamic hysteresis loops. This lumped circuit model for a nonlinear inductor is introduced into the simulation models for typical nonlinear circuits, whose dynamic hysteresis loops as well as current responses are calculated and compared with experimental measurements. Good agreement is obtained.

0. Nomenclature

A cross-sectional area normal to the flux path,
B magnetic flux density [Wb/m^2],
C capacitance [F],
D mean length of flux path,
dl infinitesimally small distance along the flux path,
E $\{e, 0\}$, voltage vector,
F $\{Ne/r, 0\}$, magnetomotive force vector,
G electric conductance matrix,
H magnetic field intensity [AT/m],
i $i_\mu + i_s$, current flowing through the coil,
i_s current due to the hysteresis loss,
i_μ magnetizing current,
L N^2/R_m, inductance [H],
M magnetic resistance matrix,
N number of turns of exciting coil,
R N^2/S_m, electric resistance [Ω],
R_m $D/(\mu A)$, magnetic resistance,
r electric resistance of coil [Ω],
r_d diode,
r_f electric resistance of the free wheeling diode [Ω],
r_r electric resistance of the rectifying diode [Ω],
S magnetic hysteresis parameter matrix,
S_m magnetic hysteresis parameter,
s hysteresis coefficient [Ω/m],
t time [sec],
v_C terminal voltage of capacitor C,
v terminal voltage of resistance R,
W $[N, N]^t$, winding matrix,
Φ $\{\phi, v_C\}$, magnetic flux vector,
ϕ magnetic flux [Wb],
Δt stepwidth in time [sec],
μ magnetic permeability [H/m],

Subscripts t, $t + \Delta t$ refer to the time t, $t + \Delta t$, respectively. Superscripts $(K + 1)$, (K), $(K - 1)$ refer to the number of iterations; and t denotes the transpose of matrix.

1. Introduction

In the design and simulation of electric circuits containing hysteresis elements it is necessary to work out a lumped circuit model that simulates closely the hysteresis phenomenon. In conventional circuit theory there are three basic types of passive elements: (1) resistances that dissipate electric energy as heat; (2) inductances that store magnetic field energy; and (3) capacitances that store electric field energy. The hysteresis phenomenon occurs notably in the inductances and capacitances. In other words, the hysteresis phenomenon always occurs in the elements storing field energy. Some part of stored energy in the electric or magnetic field will be lost when the energy flows out from the inductances or capacitances, and this energy loss is called as hysteresis loss. Depending upon the circumstances, it may be sufficient to assume that the hysteresis loss can be represented in terms of a resistance loss. However, it is most difficult to construct a model having the accuracy for analysis of nonlinear circuits such as the ferroresonant circuit [1].

Chua and Stromsmoe worked out the hysteresis model for electronic circuit studies [2]. Talukdar and Bailey worked out the hysteresis model for system studies [3]. Their model is based on the fact that the trajectory λ (magnetic flux linkage)–i (exciting current) is uniquely determined by the last point at which the flux linkage derivative $\mathrm{d}\lambda/\mathrm{d}t$ changed sign. However, the parameters of their model are determined by the set of λ–i trajectories, and this makes their model useless for the wide range problems. A recent paper has proposed a model for magnetodynamic fields taking into account dynamic hysteresis loops are predicting three-dimensional magnetodynamic fields in electromagnetic devices [4]. The parameters of this model are determined by the set of $\lambda - i$ trajectories as well as the set of $(\mathrm{d}\lambda/\mathrm{d}t)$–$i$ trajectories.

The principal purpose of this paper is to work out a lumped circuit model for a nonlinear inductor exhibiting dynamic hysteresis loops from the magnetic field equation, and to demonstrate the effects of dynamic hysteresis phenomena in the typical nonlinear circuits. The voltage across a capacitor is commonly assumed as being linearly independent; in other words, the capacitance is assumed to be constant. In practice, this is usually closely true, and at least much more so than the assumption of linear inductance for devices involving stored magnetic energy.

In order to check up the validity of our nonlinear inductor model we examine a simple R-L series electric circuit. As an example of the nonlinear oscillations in electric circuits we apply our nonlinear inductor model to the R-L-C series ferroresonant circuit. Moreover, as a practical example, our nonlinear inductor model is applied to the half wave rectifier circuit with a free wheeling diode.

2. Modeling of a nonlinear inductor

A magnetic field equation taking into account dynamic hysteresis loops is given by

$$H = \frac{1}{\mu} B + \frac{1}{s} \frac{\mathrm{d}B}{\mathrm{d}t} \tag{1}$$

where H, B, μ, s and t denote the magnetic field intensity, magnetic flux density, magnetic

permeability, magnetic hysteresis coefficient and time, respectively. For further details of (1) you may refer to Appendix A. In order to derive the lumped circuit model for a nonlinear inductor consider a simple toroidal inductor as shown in Fig. 1(a). By considering (1) and Fig. 1(a) it is possible to write the following equation

$$\int_0^D H \, \mathrm{d}l = \int_0^D \left[\frac{1}{\mu} B + \frac{1}{s}\frac{\mathrm{d}B}{\mathrm{d}t}\right]\mathrm{d}l \tag{2}$$

where D and $\mathrm{d}l$ denote the mean length of magnetic flux path and infinitesimally small distance along the magnetic flux path D, respectively. With A denoting the cross-sectional area normal to the flux path the relationship between magnetic flux density B and magnetic flux ϕ is given by

$$B = \phi / A \, . \tag{3}$$

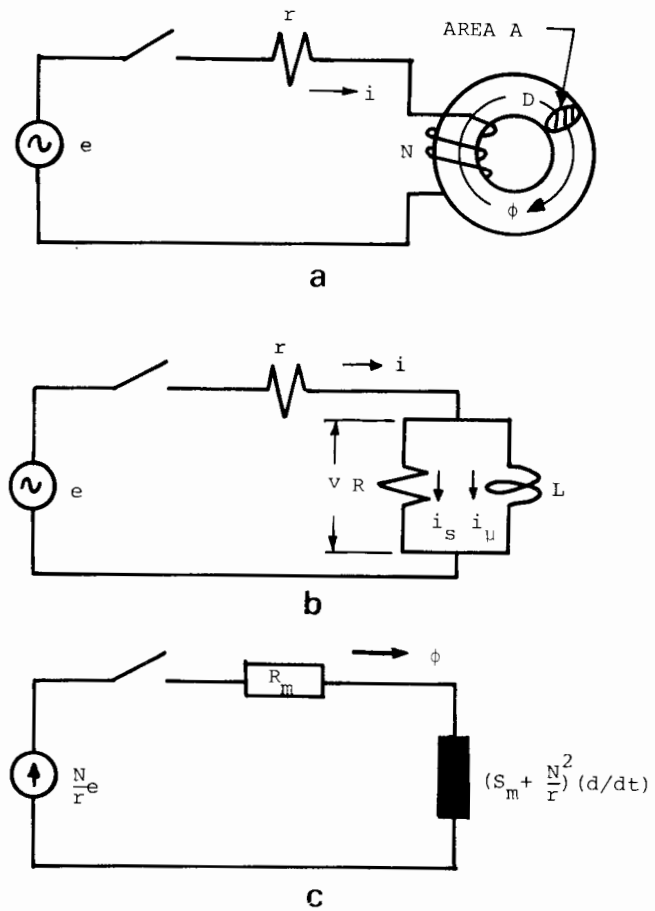

Fig. 1. A model for a nonlinear inductor. (a) Schematic diagram of a toroidal inductor; (b) electric circuit model for an inductor; (c) magnetic circuit model for an inductor.

By means of (3) the right-hand term in (2) can be rewritten as

$$\int_0^D \left[\frac{1}{\mu} B + \frac{1}{s}\frac{dB}{dt}\right] dl = R_m \phi + S_m \frac{d\phi}{dt} \tag{4}$$

where the magnetic resistance R_m and magnetic hysteresis parameter S_m are defined by

$$R_m = D/\mu A\,, \tag{5}$$

$$S_m = D/sA\,. \tag{6}$$

Moreover the left-hand term in (2) can be represented in terms of the impressed voltage e, electric resistance of coil r, magnetic flux ϕ and number of turns of coil N, that is

$$\int_0^D H\, dl = \frac{N}{r}\left[e - N\frac{d\phi}{dt}\right]. \tag{7}$$

By substituting (4) and (7) into (2), it is possible to write the following relation

$$\frac{N}{r}\left[e - N\frac{d\phi}{dt}\right] = R_m \phi + S_m \frac{d\phi}{dt}\,. \tag{8}$$

By considering the magnetic circuit equation (8) and Fig. 1(a) it is possible to derive the lumped electric circuit model for a nonlinear inductor as shown in Fig. 1(b). Since the currents i_μ and i_s in Fig. 1(b) are respectively corresponding to the terms $(1/N)R_m\phi$ and $(1/N)S_m(d\phi/dt)$ in (8), the inductance L and resistance R in Fig. 1(b) can be represented in terms of magnetic resistance R_m, magnetic hysteresis parameter S_m and number of turns of exciting coil N, that is,

$$L = \frac{N\phi}{(1/N)R_m\phi} = \frac{N^2}{R_m}, \tag{9}$$

$$R = \frac{N(d\phi/dt)}{(1/N)S_m(d\phi/dt)} = \frac{N^2}{S_m}\,. \tag{10}$$

Moreover the current i in Fig. 1(b) can be represented by

$$i = i_\mu + i_s = (1/N)[R_m\phi + S_m d\phi/dt]\,. \tag{11}$$

By considering (8)–(11) it is possible to write the integral form of nonlinear inductor model as

$$\frac{e}{r} = \left[\frac{1}{r} + \frac{1}{R}\right]v + \frac{1}{L}\int_0^t v\, dt \tag{12}$$

where the voltage v is the terminal voltage of R as shown in Fig. 1(b). On the other hand, by rearranging (8) the differential form of the nonlinear inductor model can be written as

$$(N/r)e = R_m\phi + [S_m + N^2/r]\,\mathrm{d}\phi/\mathrm{d}t\,. \tag{13}$$

By means of (13) it is possible to draw the magnetic circuit model for a nonlinear inductor as shown in Fig. 1(c). The electric circuit model for a nonlinear inductor (Fig. 1(b)) coincides with Chua's one [2].

3. Numerical method of solution

As shown in Appendix A, the magnetic permeability μ and magnetic hysteresis coefficient s in (1) are, respectively, the functions of magnetic field intensity B/μ and $(1/s)(\mathrm{d}B/\mathrm{d}t)$. Since the relationship between flux density B and magnetic flux ϕ is given by (3), the magnetic permeability μ and magnetic hysteresis coefficient s are formally represented by

$$\mu = f_\mu(\phi)\,, \tag{14}$$

$$s = f_s(\mathrm{d}\phi/\mathrm{d}t)\,, \tag{15}$$

where $f(\cdot)$ denotes the single valued function of $(\cdot)$. As shown in (14) and (15) the nonlinear parameters μ and s are directly related to the magnetic flux ϕ, therefore it is preferable to use the magnetic circuit model of a nonlinear inductor. Thus, in this paper, we employed the magnetic circuit model of (13). By considering (14) and (15) the magnetic circuit equation (13) can be represented as following form

$$\mathrm{d}\phi/\mathrm{d}t = f(\phi, \mathrm{d}\phi/\mathrm{d}t, t)\,. \tag{16}$$

Equation (16) means that the magnetic circuit model of a nonlinear inductor is a nonlinear differential equation whose coefficients are the functions of the magnetic flux ϕ, the time derivative of the magnetic flux $\mathrm{d}\phi/\mathrm{d}t$ and time t.

For numerically solving (16), this nonlinear differential equation (16) is replaced by the following divided difference equation

$$(\phi_{t+\Delta t} - \phi_t)/\Delta t = f(\tfrac{1}{2}(\phi_{t+\Delta t} + \phi_t), (\phi_{t+\Delta t} - \phi_t)/\Delta t, t + \tfrac{1}{2}\Delta t) \tag{17}$$

where Δt denotes the stepwidth in time t; and subscripts $t+\Delta t$, t refer to the time $t+\Delta t$, t, respectively. With the superscripts $(K+1)$, (K), $(K-1)$ denoting the number of iterations, (17) is iteratively solved by

$$\phi_{t+\Delta t}^{(K+1)} = \phi_t + \Delta t f(\tfrac{1}{2}(\phi_{t+\Delta t}^{*} + \phi_t), (\phi_{t+\Delta t}^{*} - \phi_t)/\Delta t, t + \tfrac{1}{2}\Delta t) \tag{18}$$

where $\phi_{t+\Delta t}^{*}$ is

$$\phi_{t+\Delta t}^{*} = \phi_{t+\Delta t}^{(K-1)} + \tfrac{1}{2}[\phi_{t+\Delta t}^{(K)} - \phi_{t+\Delta t}^{(K-1)}]\,. \tag{19}$$

Fig. 2 shows the flow chart of this iteration method.

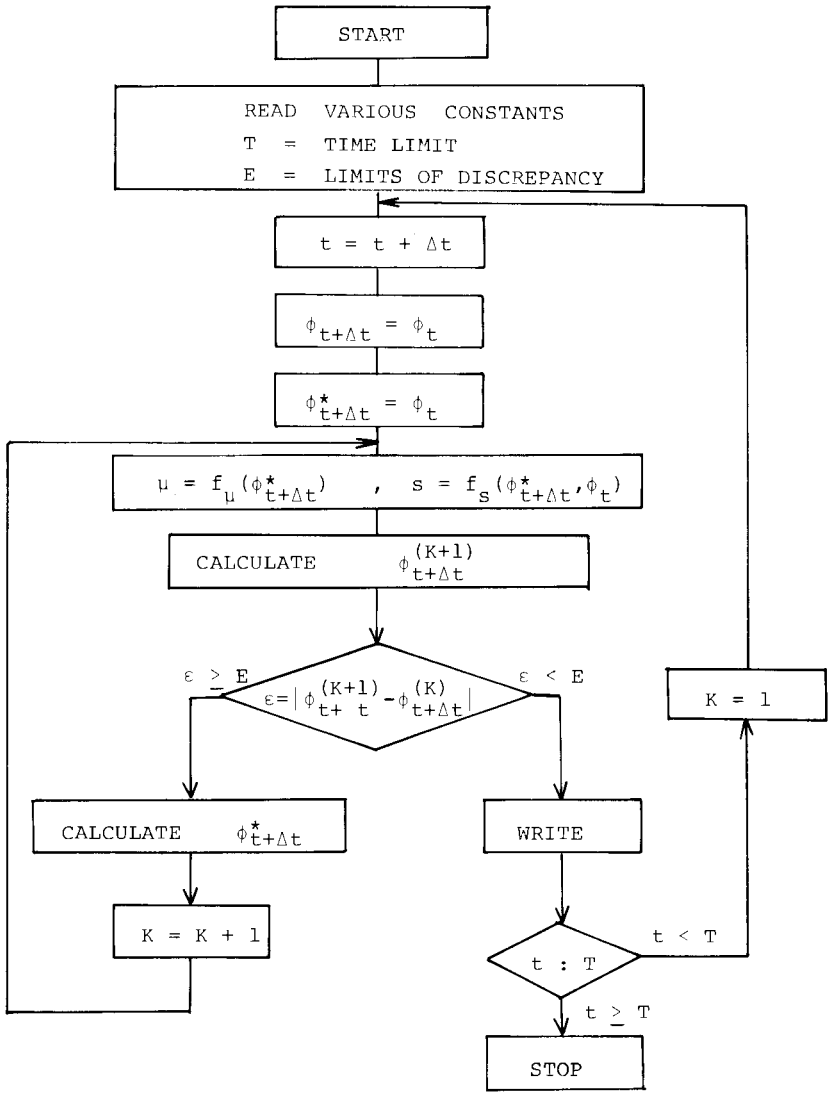

Fig. 2. Flow chart of the iteration method.

4. Numerical solutions

(1) *R-L series circuit.* In order to check up the validity of the lumped circuit model for a nonlinear inductor we examined a simple *R-L* series circuit. In this case, the schematic diagram, electric circuit model and magnetic circuit model are essentially similar in Figs. 1(a), 1(b) and 1(c), respectively. By rearranging (13) the magnetic circuit equation is formally written in the form of (16) as

$$(\mathrm{d}/\mathrm{d}t)\phi = -[S_m + (N^2/r)]^{-1}[R_m\phi - (N/r)e]\,. \tag{20}$$

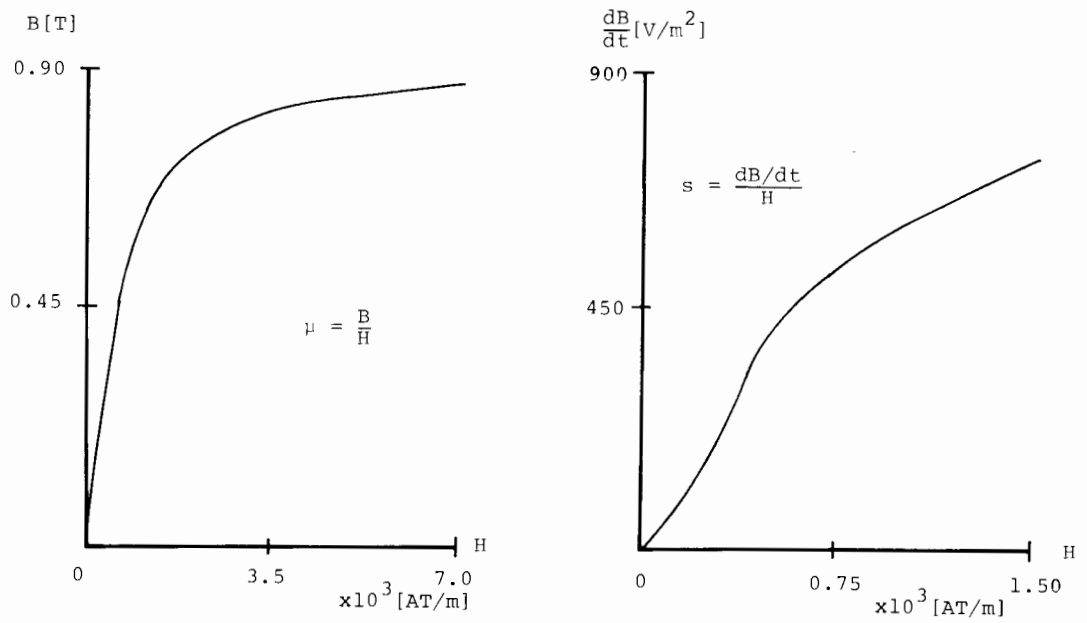

Fig. 3. Magnetization curves used in the calculations.

The magnetization curves for the magnetic permeability μ and magnetic hysteresis coefficient s in (14) and (15) are shown in Fig. 3. In carrying out the calculations these curves are represented by linear interpolation. The stepwidth Δt in (17)–(19) was determined as $\Delta t \leq 0.25$ [msec] by the numerical tests when the convergence and accuracy of the solutions were taken into account. Various constants used in the calculations are listed in Table 1.

Table 1
Various constants used in the calculations; all the initial magnetic flux and current are set to zero

Toroidal inductor	
Area normal to the flux path	$A = 0.0001$ [m^2]
Mean length of magnetic flux path	$D = 0.2827$ [m]
R-L series circuit	
Number of turns of coil	$N = 900$ [turns]
Electric resistance of coil	$r = 6.30$ [Ω]
R-L-C series ferroresonant circuit	
Number of turns of coil	$N = 1500$ [turns]
Electric resistance of coil	$r = 16.4$ [Ω]
Capacitance	$C = 50.0$ [μF]
Half wave rectifier circuit	
Number of turns of coil	$N = 800$ [turns]
Electric resistance of coil	$r = 5.86$ [Ω]
Limit of discrepancy	$\varepsilon = 0.001$ [percent]

Fig. 4(a) shows the steady state dynamic hysteresis loops when the three different voltages with frequency 50 [Hz] are impressed. Fig. 4(b) shows the transient state dynamic hysteresis loops as well as currents flowing through the coil. Moreover, comparisons of experimental and computational results were made for the transient state values when the impressed voltage contained a fifth harmonic wave. The results are shown in Fig. 4(c). Because of the difficulty in obtaining a good supply voltage wave containing a fifth harmonic wave, the discrepancies between the experimental and computational results are not necessarily as small as those of Figs. 4(a) and 4(b).

(2) *R-L-C series ferroresonant circuit.* The circuit containing a nonlinear inductor leads to nonlinear phenomena [1]. As an example of the nonlinear phenomena we examined a *R-L-C* series ferroresonant circuit. The schematic diagram, electric circuit model and magnetic circuit model of this case are shown in Figs. 5(a), 5(b) and 5(c), respectively. In this case, the magnetic circuit equation becomes to a system of equations involving the magnetic flux vector Φ, the externally impressed magnetomotive force vector F, the magnetic resistance matrix M and the magnetic hysteresis parameter matrix S, that is,

$$(\mathrm{d}/\mathrm{d}t)\Phi = -S^{-1}[M\Phi - F] \tag{21}$$

where

$$\Phi = \{\phi, v_C\}, \tag{22}$$

$$F = \{(N/r)e, 0\}, \tag{23}$$

$$M = \begin{bmatrix} R_m & N/r \\ R_m & 0 \end{bmatrix}, \tag{24}$$

$$S = \begin{bmatrix} S_m + (N^2/r) & 0 \\ S_m & -NC \end{bmatrix}. \tag{25}$$

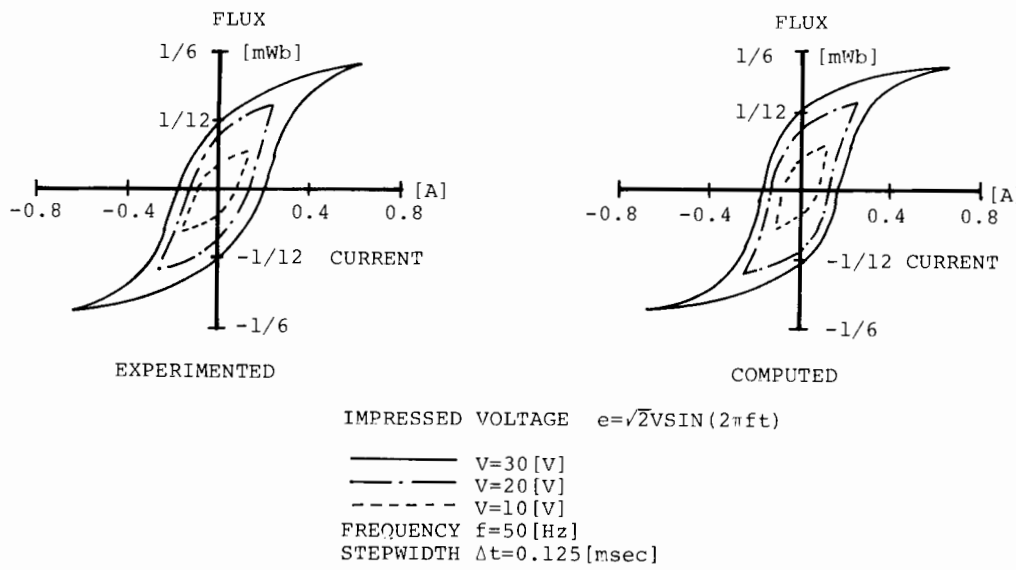

Fig. 4(a). Steady state dynamic hysteresis loops of *R-L* series circuit.

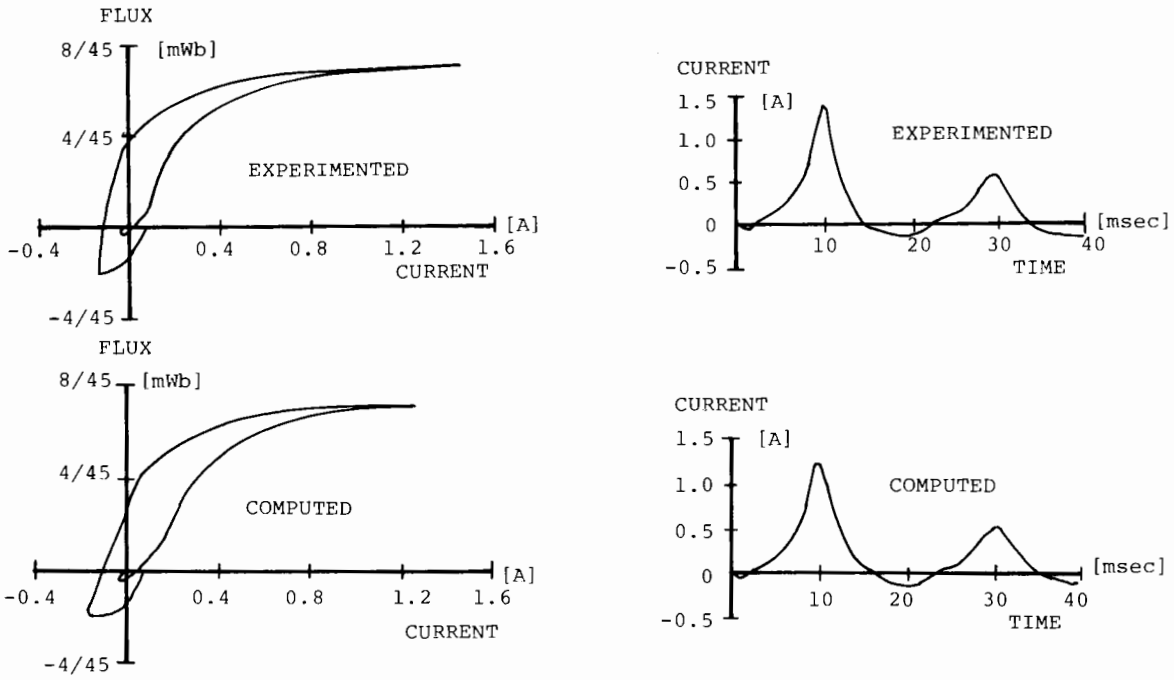

IMPRESSED VOLTAGE $e=\sqrt{2}V\sin(2\pi ft+\Psi)$, V=20[V], f=50[Hz], Ψ=-21.4[deg.]
STEPWIDTH Δt=0.125[msec]

Fig. 4(b). Transient state dynamic hysteresis loops and currents of *R-L* series circuit.

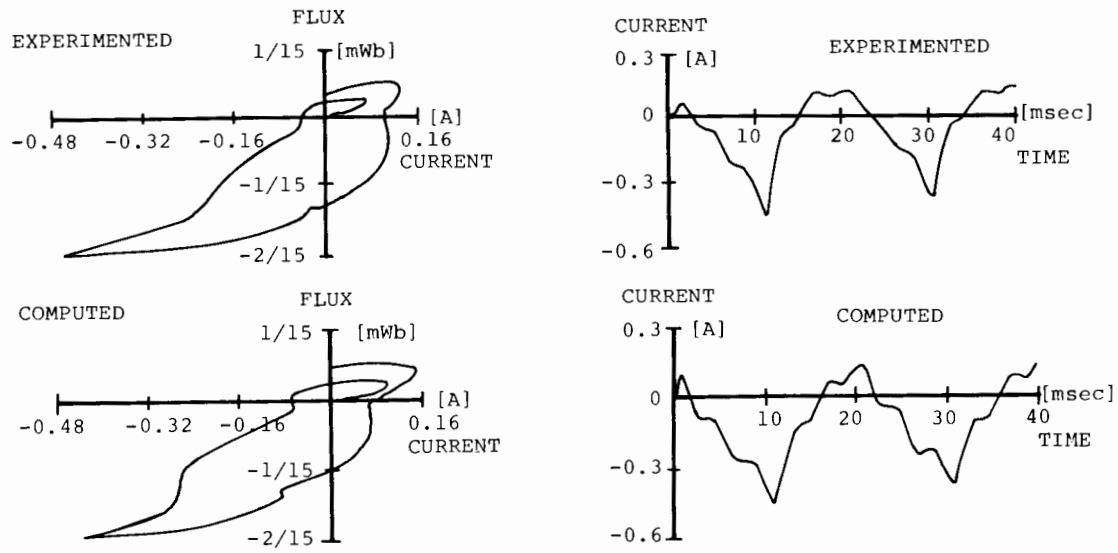

IMPRESSED VOLTAGE $e=\sqrt{2}V\{\sin(2\pi ft+\Psi)+(1/2)\sin[5(2\pi ft+\Psi)]\}$, V=15[V], f=50[Hz], Ψ=153[deg.]
STEPWIDTH Δt=0.1[msec]

Fig. 4(c). Transient state dynamic hysteresis loops when the impressed voltage contains a fifth harmonic wave.

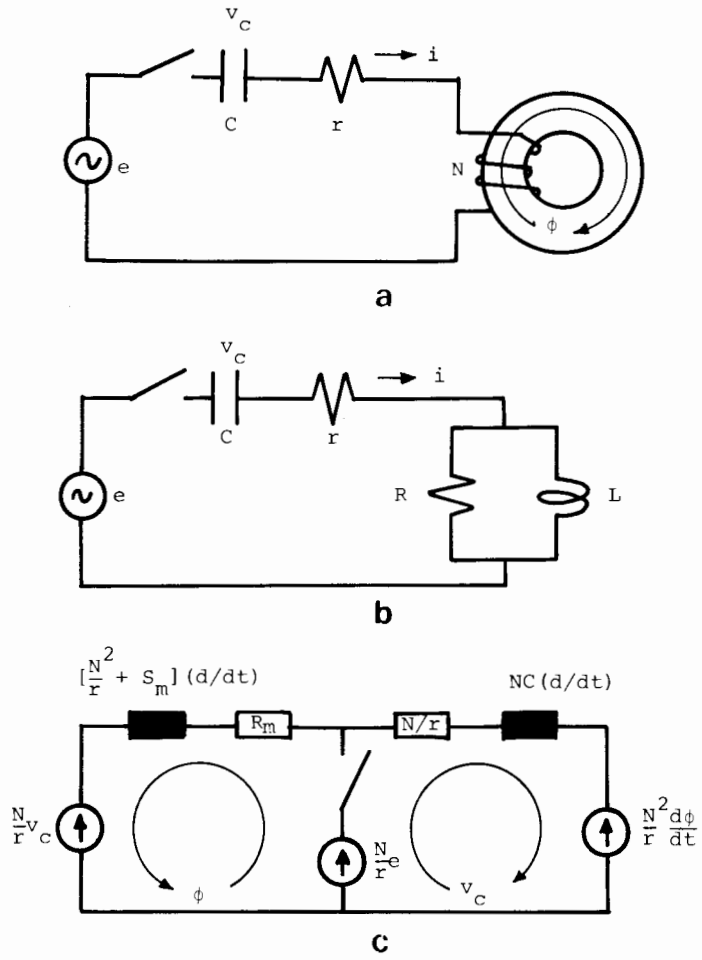

Fig. 5. Modeling of a ferroresonant R-L-C series circuit. (a) Schematic diagram; (b) electric circuit model; (c) magnetic circuit model.

In (22) the terminal voltage of capacitance C is denoted by v_C.

In order to get the resonant frequency about 25 [Hz] associated with the maximum magnetic permeability we selected the capacitance $C = 50$ [μF] and number of turns of coil $N = 1500$ [turns]. This selection of number of turns of coil made the electric resistance of coil $r = 16.4$ [Ω]. Various constants used in the calculations are summarized in Table 1.

Both calculations and experimentations were carried out under the transient state when three different voltages with amplitude of 40, 35, 30 [V] were impressed on the R-L-C series ferroresonant circuit. Ferroresonant oscillation always occurred by the voltage with amplitude of 40 [V], but never occurred by the voltage with amplitude of 30 [V]. Ferroresonant oscillation occurred by the phase angle $\Psi = 35.1$ [deg] of voltage with amplitude of 35 [V] as shown in Fig. 6(a). However, as shown in Fig. 6(b), ferroresonant oscillation did not occur by the phase angle $\Psi = 53.4$ [deg] of voltage with amplitude of 35 [V]. Therefore, when the voltage with amplitude of 35 [V] is impressed, ferroresonant oscillation depends on the phase angle of input voltage.

(3) *The half wave rectifier circuit with a free wheeling diode.* As a practical application of our lumped circuit model for a nonlinear inductor we applied our model to the half wave rectifier circuit with a free wheeling diode. This example is very useful and interesting for studying the dynamic hysteresis phenomena, because this example produces the minor hysteresis loops under the transient state, and current flowing through the coil of the inductor never takes negative values.

The schematic diagram, electric circuit model and magnetic circuit model of this case are shown in Figs. 7(a), 7(b) and 7(c), respectively. The diode r_d in Fig. 7(a) is introduced into the rectifier circuit models of Figs. 7(b) and 7(c) as a nonlinear resistance whose terminal characteristic curve is shown in Fig. 8. Since the current (which is the horizontal axis of Fig. 8) is a function of magnetic flux ϕ, the time derivative of magnetic flux $d\phi/dt$ and time t, the diode r_d is reduced to a function of ϕ, $d\phi/dt$ and t. In carrying out the calculations the resistance of diode r_d is represented in linear interpolation. Depending upon the operating conditions the resistance of diode r_d takes a different value. Therefore, in Figs. 7(b) and 7(c) the diode operating as a rectifier and a free wheeling diode are denoted by r_r and r_f,

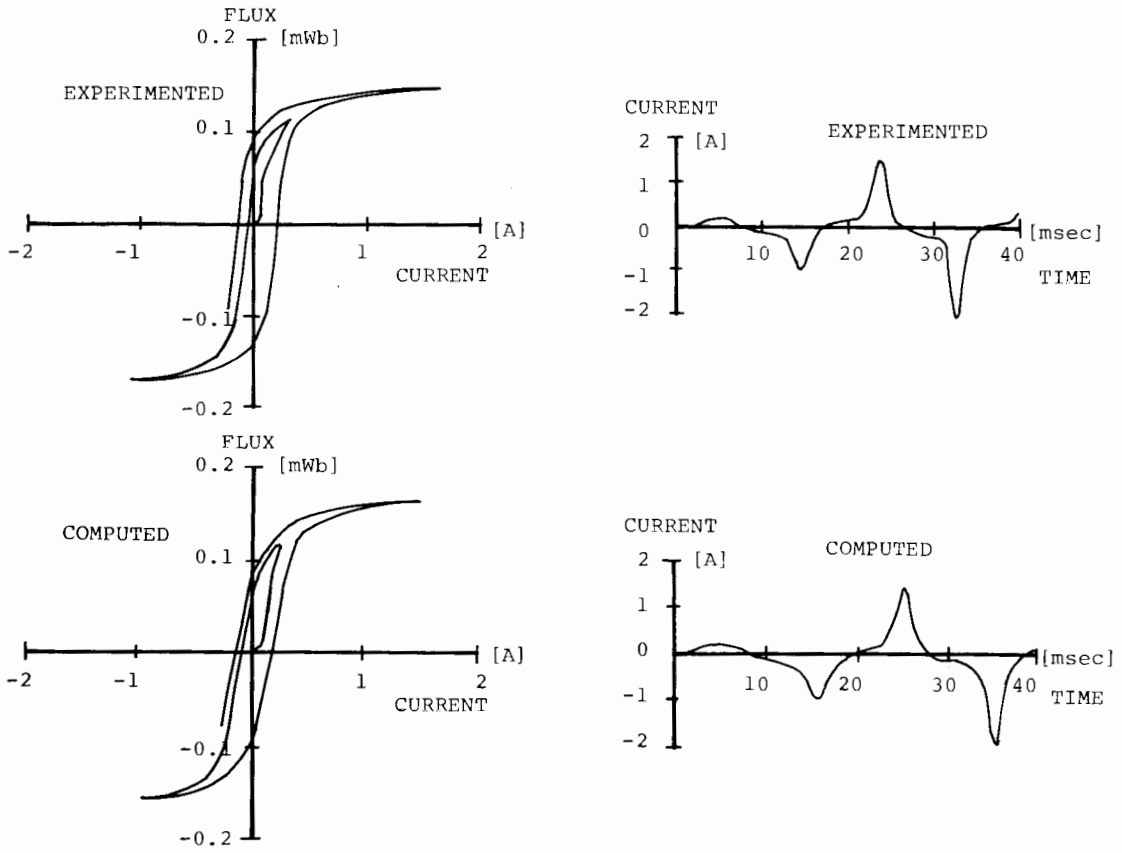

IMPRESSED VOLTAGE $e=\sqrt{2}V\sin(2\pi ft+\Psi)$, V=35[V], f=50[Hz], Ψ=35.1[deg.]

STEPWIDTH Δt=0.25[msec]

Fig. 6. Dynamic hysteresis loops and currents of ferroresonant *R-L-C* series circuit.

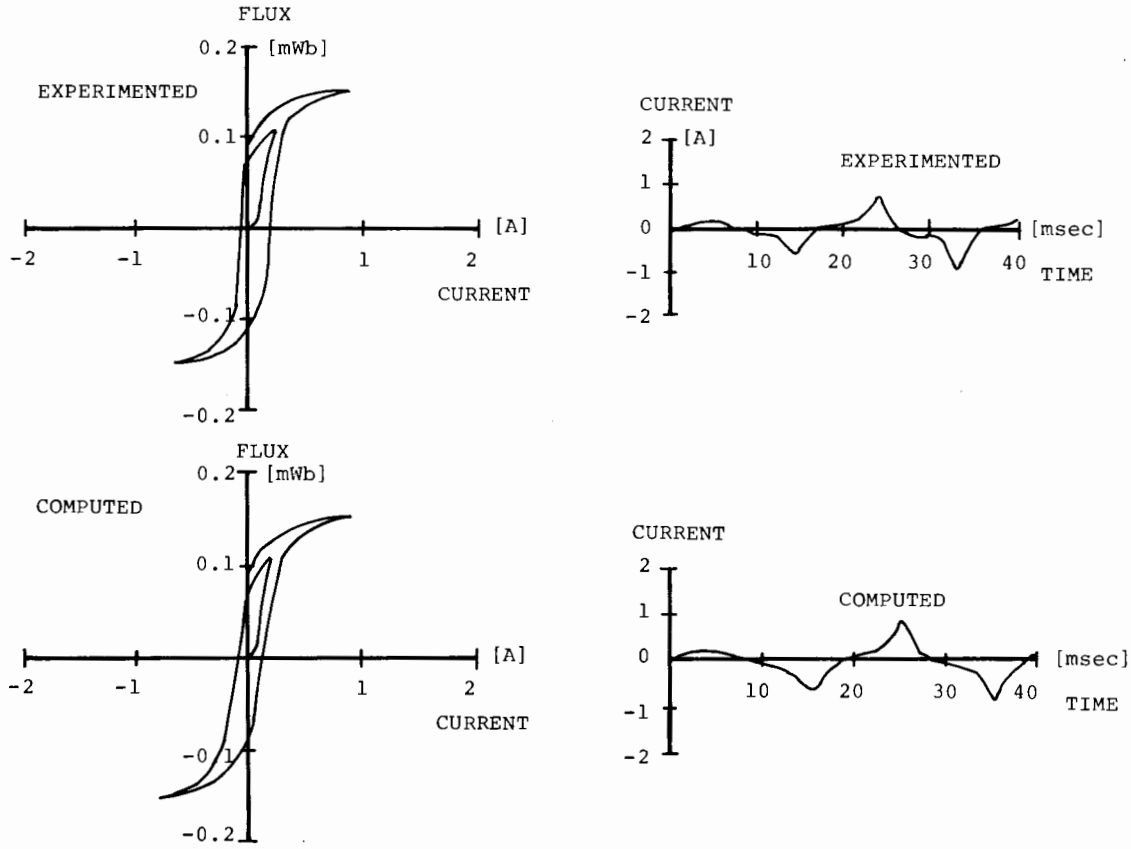

IMPRESSED VOLTAGE $e=\sqrt{2}V\sin(2\pi ft+\Psi)$, V=35[V], f=50[Hz], Ψ=53.4[deg.]
STEPWIDTH Δt=0.25[msec]

Fig. 6. Contd.

respectively. The magnetic circuit equation involving the winding matrix W, the electric conductance matrix G and the voltage vector E is written by

$$(\mathrm{d}/\mathrm{d}t)\phi = -[S_m + W^t G W]^{-1}[R_m\phi - W^t G E] \tag{26}$$

where

$$W = [N, N]^t, \tag{27}$$

$$G = \begin{bmatrix} r + r_r & r \\ r & r + r_f \end{bmatrix}^{-1}, \tag{28}$$

$$E = \{e, 0\}. \tag{29}$$

Various constants used in the calculations are listed in Table 1. Fig. 9(a) shows the dynamic hysteresis loops containing minor loops and transient currents flowing through the coil. Fig. 9(b) shows the steady state dynamic hysteresis loops and currents.

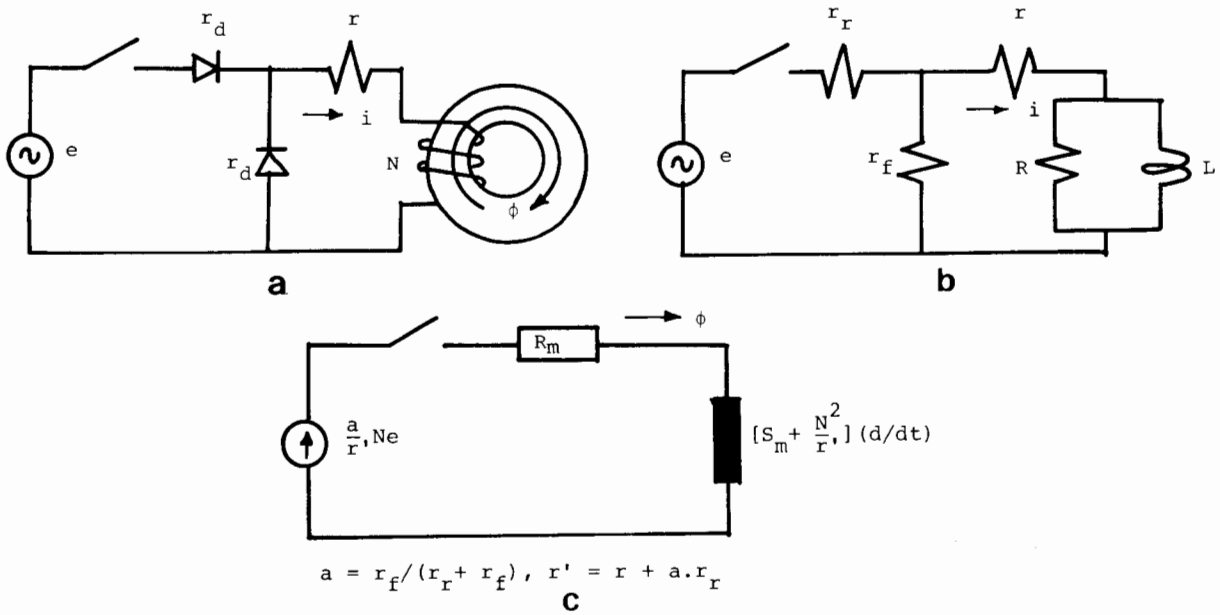

Fig. 7. Modeling of a half wave rectifier circuit with a free wheeling diode. (a) Schematic diagram; (b) electric circuit model; (c) magnetic circuit model.

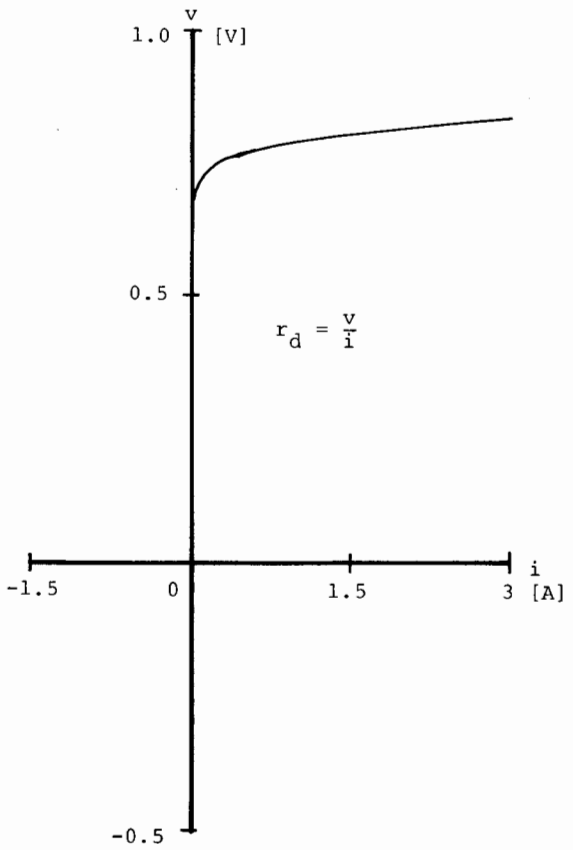

Fig. 8. Terminal characteristic curve of the diode.

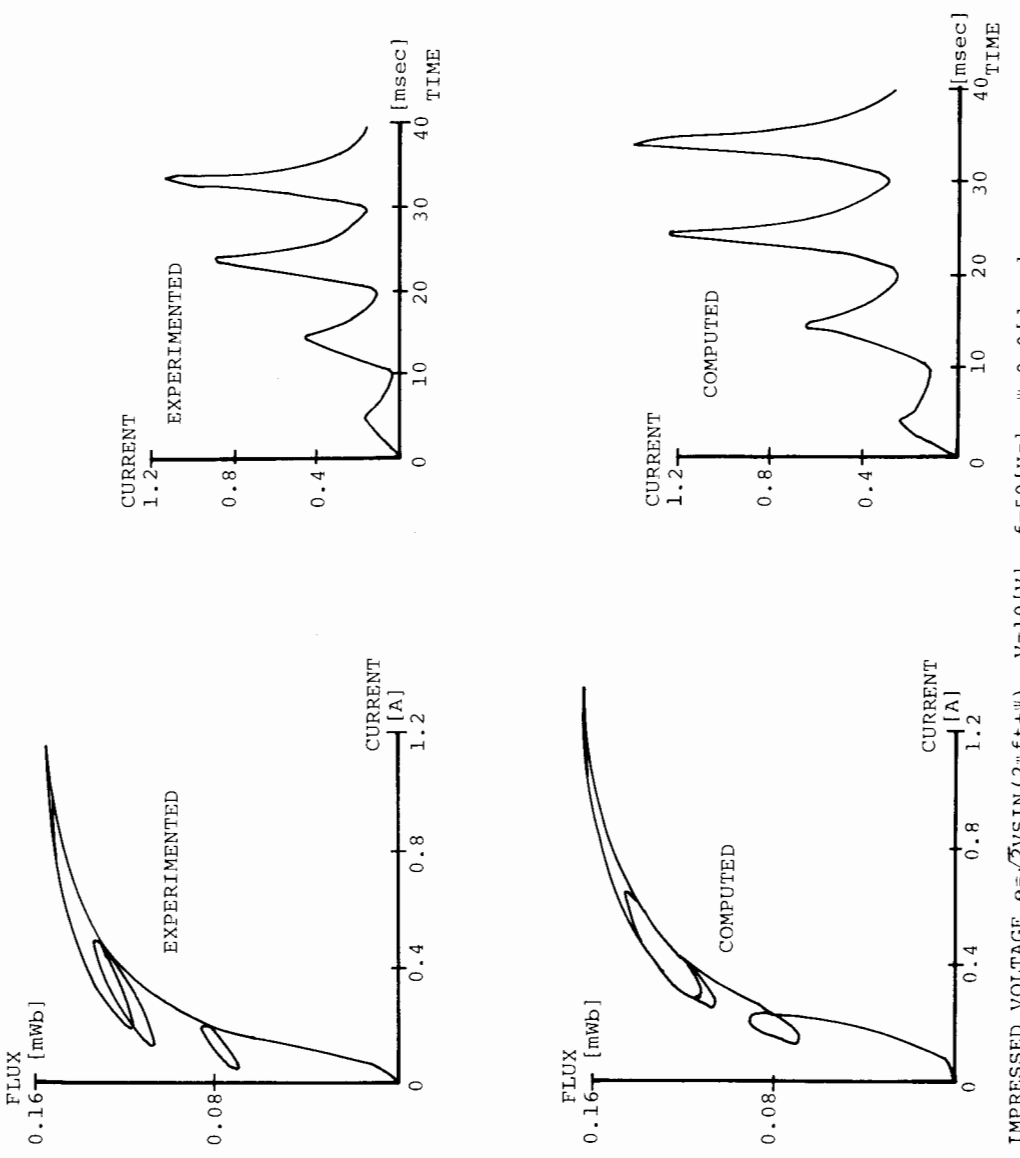

Fig. 9(a). Transient state dynamic hysteresis loops and currents of the half wave rectifier circuit with a free wheeling diode.

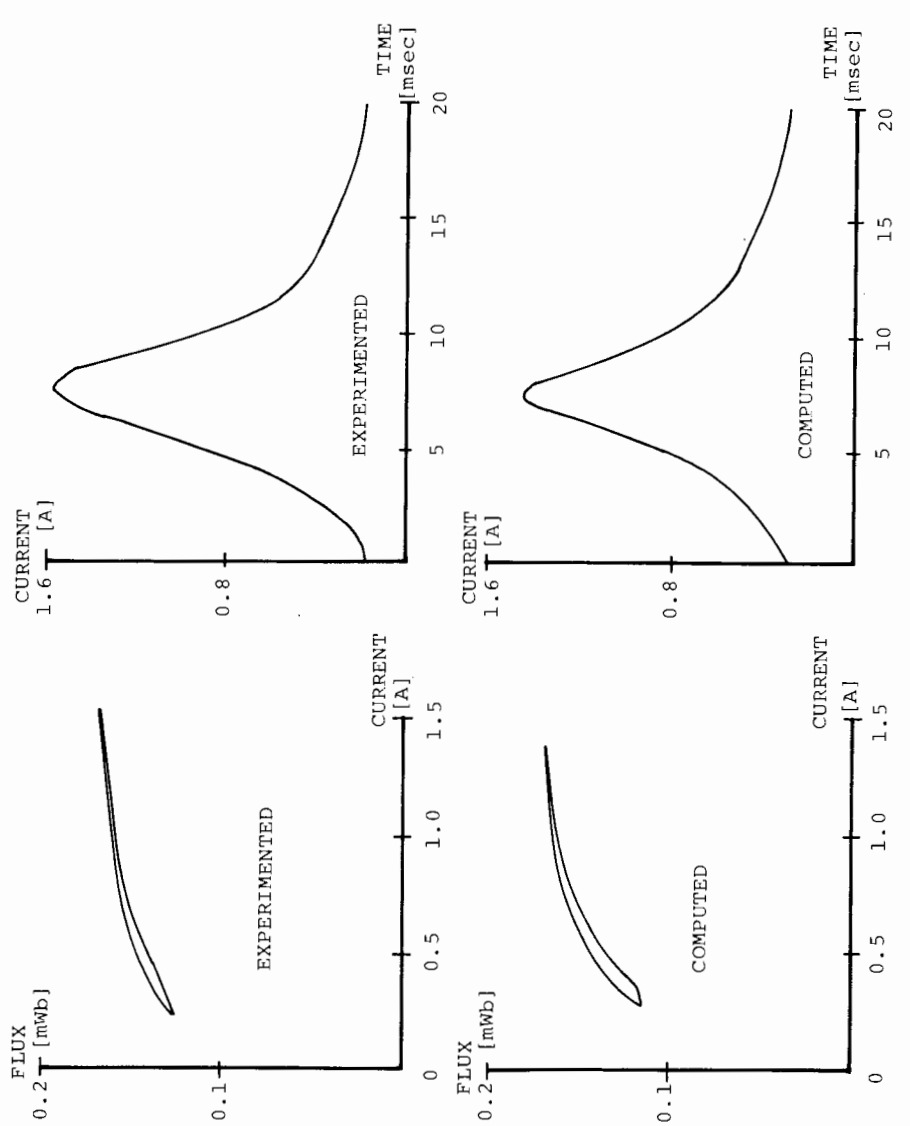

Fig. 9(b). Steady state dynamic hysteresis loops and currents of the half wave rectifier circuit with a free wheeling diode.

5. Conclusion

As shown we have derived one specific nonlinear inductor model exhibiting dynamic hysteresis loops, and demonstrated its applicability to the nonlinear electric circuits. Particularly, our magnetic circuit approach has enabled us to simulate the nonlinear circuit containing diodes without considering their switching problems [5]. This means that it may be possible to work out a computerized design of power electronic circuits. For further study, the authors plan to work out the digital simulation of a single phase parallel inverter.

The time required to obtain the results of Fig. 9(a) was about 20 minutes on the Micro Computer SORD M243 Mark 4 (Z80A CPU).

Appendix A. A magnetic field equation exhibiting dynamic hysteresis loops

Fig. 10(a) shows a typical magnetic hysteresis loop. When we consider an arbitrary point (H_a, B_a) in Fig. 10(a), it is possible to consider that the magnetic field intensity H_a is composed

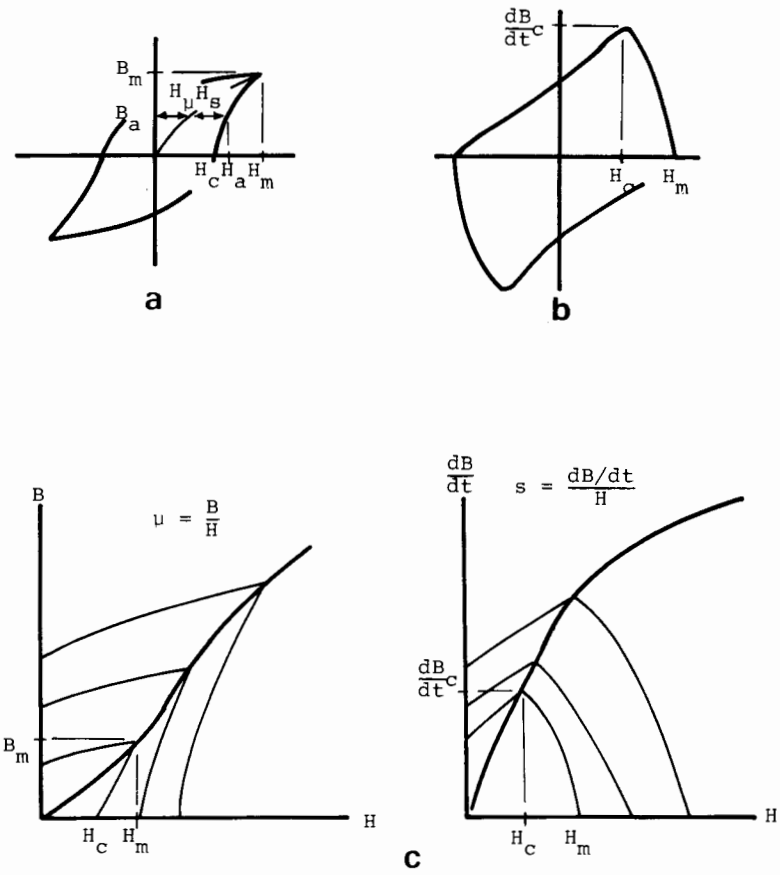

Fig. 10. Modeling the magnetic field equation taking into account dynamic hysteresis loops. (a) A typical hysteresis loop; (b) the relationship between dB/dt and H; (c) the construction of magnetization curves.

of two magnetic field intensities H_μ and H_s, that is,

$$H_a = H_\mu + H_s . \tag{A.1}$$

The relationship between the magnetic field intensity H_μ and magnetic flux density B_a is assumed to take the following form

$$H_\mu = (1/\mu)B_a \tag{A.2}$$

where μ denotes the magnetic permeability of the material. When the permeability μ is introduced into (A.2) as a function of the magnetic field intensity H_μ or magnetic flux density B_a, then (A.2) represents the magnetic saturation property of the material. Therefore, the remaining term H_s in (A.1) has to represent the dynamic hysteresis property. Hence, at least, the magnetic field intensity H_s has to satisfy the following conditions: (1) when the magnetic flux density B is increasing from $-B_m$ to $+B_m$, H_s must take positive values; (2) when the magnetic flux density B is decreasing from $+B_m$ to $-B_m$, H_s must take negative values; (3) when the magnetic flux density B reaches to the positive or negative maximum value $\pm B_m$, H_s must die out; and (4) the area bounded by the hysteresis loop must be equivalent to the loss of energy per unit volume. Fig. 10(b) shows the relationship between the magnetic field intensity H and time derivative of magnetic flux density B. By considering the above conditions (1)–(4) and Figs. 10(a) and 10(b) it is possible to assume that the magnetic field intensity H_s depends on the rate of change of the magnetic flux density B_a in time t, that is,

$$H_s = \frac{1}{s}\frac{dB_a}{dt} \tag{A.3}$$

where the hysteresis coefficient s is introduced to relate H_s with dB_a/dt and has the unit of ohm per meter. The magnetic hysteresis loss of power P_a (watt per volume) at a point (H_a, B_a) in Fig. 10(a) is given by

$$P_a = H_s\left(\frac{dB_a}{dt}\right) = \frac{1}{s}\left(\frac{dB_a}{dt}\right)^2 . \tag{A.4}$$

By means of (A.1)–(A.4) the magnetic field equation exhibiting dynamic hysteresis loops is assumed to take the following form

$$H = \frac{1}{\mu}B + \frac{1}{s}\frac{dB}{dt} . \tag{A.5}$$

When we consider the peak point (H_m, B_m) in Fig. 10(a), the permeability μ_m can be calculated by $\mu_m = B_m/H_m$, because the time derivative of the magnetic flux density B in Fig. 10(b) is reduced to zero at the point (H_m, B_m) in Fig. 10(a). Also, the hysteresis coefficient s_c can be calculated by $s_c = (dB_c/dt)/H_c$, because the magnetic flux density B in Fig. 10(a) is reduced to zero at the point $(H_c, dB_c/dt)$ in Fig. 10(b). Similarly, the permeabilities and hysteresis coefficients in the other points can be obtained, and their results construct the magnetization curves as shown in Fig. 10(c).

Acknowledgment

The first planning of this paper was carried out at the Computational Analysis and Design Laboratory at McGill University where one of the authors (Saito) stayed as a visiting researcher and the other (Saotome) stayed as a visiting graduate student in electrical engineering. The authors are grateful to Professor P. Silvester, Professor Z. Csendes and Professor D. Lowther for the facilities given by them at their Laboratory.

References

[1] J.G. Santesmases, J. Ayala and H. Cachero, Analytical approximation of a dynamic hysteresis loop and its application to a series ferroresonant circuit, Proc. IEE 117(1) (1970) 234–240.
[2] L.O. Chua and K.A. Stromsmoe, Lumped-circuit models for a nonlinear inductor exhibiting hysteresis loops, IEEE Trans. Circuit Theory 17(4) (1970) 564–574.
[3] S.N. Talukdar and J.R. Bailey, Hysteresis model for system studies, IEEE Trans. Power Apparatus and Systems 95(4) (1976) 1429–1434.
[4] Y. Saito, Three-dimensional analysis of magnetodynamic fields in electromagnetic devices taken into account the dynamic hysteresis loops, IEEE Trans. Magnetics 18(2) (1982) 546–551.
[5] A.E. Fitzgerald, C. Kingsley and A. Kusko, Electric Machinery (McGraw-Hill, New York, 1971).